PROCEEDINGS OF SPIE

SPIEDigitalLibrary.org/conference-proceedings-of-spie

Suppression of indium clustering and quantum confined stark effect of InGaN LED on silicon (111)

Richard Liu, Callan McCormick, Can Bayram

Richard Liu, Callan McCormick, Can Bayram, "Suppression of indium clustering and quantum confined stark effect of InGaN LED on silicon (111)," Proc. SPIE 10918, Gallium Nitride Materials and Devices XIV, 1091822 (1 March 2019); doi: 10.1117/12.2506426

SPIE.

Event: SPIE OPTO, 2019, San Francisco, California, United States

Suppression of indium clustering and quantum confined stark effect of InGaN LED on Silicon (111)

Richard Liu, Callan McCormick, Can Bayram
Dept. of Electrical and Computer Engineering, 306 N Wright St, Urbana, IL, USA 61801
Micro and Nanotechnology Laboratory, 208 N Wright St, Urbana, IL, USA 61801

ABSTRACT

Optical properties of InGaN/GaN multi-quantum-well (MQWs) grown on sapphire and on Si(111) are reported. The tensile strain in the MQW on Si is shown to be beneficial for indium incorporation and Quantum-confined Stark Effect reduction in the multi-quantum wells. Raman spectroscopy reveals compressive strains of -0.107% in MQW on sapphire and tensile strain of +0.088% in MQW on Si. Temperature-dependent photoluminescence shows in MQW on sapphire a strong (30 meV peak-to-peak) S-shaped wavelength shift with decreasing temperature (6 K to 300K), whereas MQW on Si luminescence wavelength is stable and red-shifts monotonically. Micro-photoluminescence mapping over 200 by 200 μm^2 shows the emission wavelength spatial uniformity of MQW on Si is 2.6 times higher than MQW on sapphire, possibly due to a more uniform indium incorporation in the multi-quantum-wells as a result of the tensile strain in MQW on Si. A positive correlation between emission energy and intensity is observed in MQW on sapphire but not in those on Si. Despite the lower crystal quality of MQW on Si revealed by atomic force microscopy, it exhibits a higher internal quantum efficiency (IQE) than MQW on sapphire from 6 K to 250 K, and equalizes at 300 K. Overall, MQW on Si exhibits a high IQE, higher wavelength spatial uniformity and temperature stability, while providing a much more scalable platform than MQW on sapphire for next generation integrated photonics.

Keywords: MQW, Silicon, MOCVD, AlGaN buffer layer, IQE, indium incorporation, quantum confined stark effect

1. INTRODUCTION

Recent advances in the solid-state lighting has enabled light emitting diodes (LEDs) based on the Indium gallium nitride (InGaN) / gallium nitride (GaN) multiple quantum wells (MQW) to transform the general lighting market by the virtue of the efficiency, ruggedness, and compactness of the semiconductor. Despite their clear advantages over the conventional technologies, adoption of LEDs is hindered by the high upfront cost, which is caused by a combination of expensive substrates, lack of scalability, and epitaxial difficulties. Due to the lack of commercially viable native substrates, conventional GaN-based LEDs to be heterogeneously grown on foreign substrates such as sapphire (Al_2O_3), which has a -16% lattice mismatch with GaN.[1] Another approach is to grow these devices on Si(111) substrates. The advantages of this platform include affordable and large diameter substrates, existing Si processing technologies, and the possibility of integration with Si devices. Using Si substrates can potentially significantly reduce the initial cost of device, and thus increase the adoption rate and market share of solid-state lighting.[2]

The biggest challenge of this approach comes from the very large lattice (+17%) and thermal expansion coefficient (-115%) mismatch between GaN epilayer and the Si substrate. These mismatches have been mitigated by the use of stress managing AlGaN buffer layers, AlN interlayers, or engineered substrates.[3–7] These growth technologies have enabled LED on Si(111) to achieve an level of performance that is on par with LED on Al_2O_3.[8] However, carrier dynamics in the InGaN quantum wells have not been thoroughly compared between these two platforms, especially since they exhibit the opposite kinds of residual strain. Literature has reported that the strain plays a significant role in the incorporation of indium atoms in the InGaN layers.[9,10] In this work, blue-emitting MQW layers are grown on c-plane Al_2O_3 (MQW-Al_2O_3) and Si(111) (MQW-Si) substrates. Structural studies using Raman spectroscopy and atomic force microscopy (AFM), and optical studies using micro-photoluminescence (micro PL), temperature-dependent PL are carried out in order to compare the carrier dynamics in MQWs on Al_2O_3 and Si substrates.

Gallium Nitride Materials and Devices XIV, edited by Hiroshi Fujioka, Hadis Morkoç,
Ulrich T. Schwarz, Proc. of SPIE Vol. 10918, 1091822 · © 2019 SPIE
CCC code: 0277-786X/19/$18 · doi: 10.1117/12.2506426

2. EXPERIMENT

Figure 1 shows the cross section scanning electron microscopy images of (a) MQW-Al_2O_3 and (b) MQW-Si grown by metalorganic chemical vapor deposition (MOCVD). Six pairs of 2-nm thick $In_{0.15}Ga_{0.85}N$ / 13-nm thick GaN are deposited. The overall thickness of the epitaxial layers of MQW-Si (3.3 µm), including the AlGaN buffer layers, is thinner than that of MQW-Al_2O_3 (4.6 µm). No cracks are observed on the surface of either samples.

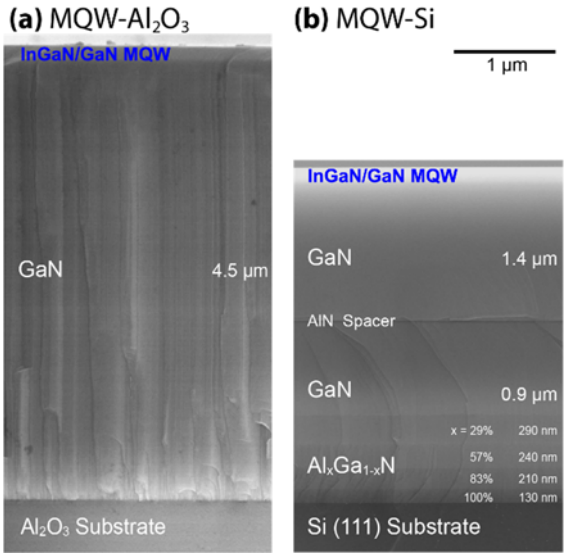

Figure 1. Cross-sectional SEM images of the MOCVD-grown (a) MQW-Al_2O_3, and (b) MQW-Si. Identical blue-emitting MQW layers are grown on both samples.

Figure 2 shows peak positions and their integrated intensities of (left) MQW-Al_2O_3 and (right) MQW-Si using a continuous wave HeCd 325 nm laser micro PL setup over a 200 µm by 200 µm area. MQW-Al_2O_3 exhibit integrated intensity uniformity of 5.1% and average peak position of 2.791 eV ± 3.7 meV. In comparison, MQW-Si shows a similar intensity distribution with a uniformity of 4.1%, and an average peak position that has a slightly higher energy at 2.823 eV with a smaller distribution of ± 1.4 meV. MQW-Al_2O_3 shows a strong and positive correlation between the peak position and intensity (R^2 = 0.75), whereas this correlation is not observed in MQW-Si (R^2 = 0.11). Comparing a typical dimmer location with a brighter one on MQW-Al_2O_3 (shows that the brighter location emits roughly the same number of photons in the low energy part of the spectrum, but more intensely in the higher energy shoulder along with a shift in peak position. This kind of intensity-energy correlation has been reported in the literature as the screening of the quantum confined stark effect (QCSE) and filling of the states in the emission centers.[11,12] The lack of this correlation in MQW-Si suggests these effects are less pronounced. Raman spectroscopy is then conducted to verify the stress of the samples to examine the origin of the differences observed in micro PL.

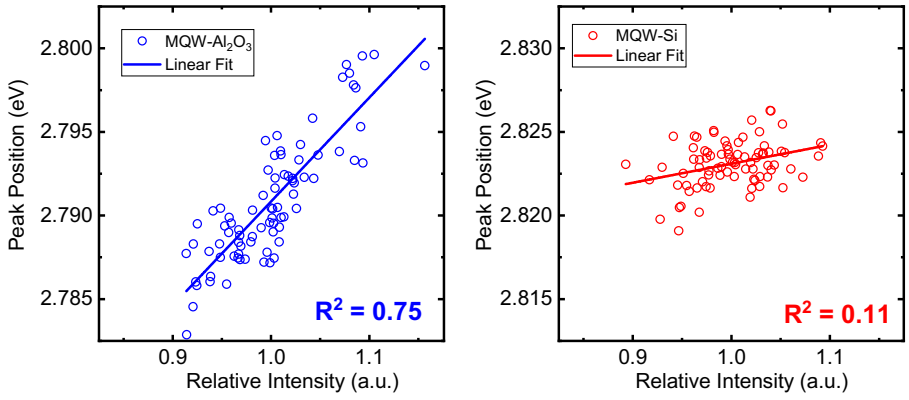

Figure 2. Micro-photoluminescence peak positions and integrated intensities of (left) MQW-Al_2O_3 and (right) MQW-Si.

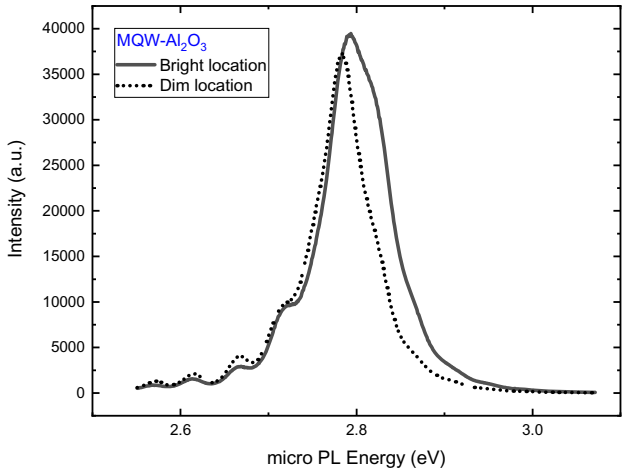

Figure 3. Micro PL spectra of a typical (solid line) bright location and a typical (dotted line) dim location on MQW-Al_2O_3.

Figure 4 shows the Raman spectroscopy of the (blue) MQW-Al_2O_3 and (red) MQW-Si. Both samples show the E_2^H phonon shift of GaN while MQW-Si shows an additional saturated peak at 520 cm^{-1}, which originates from its silicon substrate. The E_2^H Raman shift of GaN in the MQW-Al_2O_3 (569.7 cm^{-1}) exhibits a blue-shift in energy from its relaxed value (567.5 cm^{-1}); this indicates a compressive strain experienced in the GaN layer. MQW-Si exhibits the opposite shift (565.7 cm^{-1}), which indicates the presence of a tensile strain. The in-plane biaxial stress and strain are calculated using:[13]

$$\Delta\omega = 4.3\ \sigma_{xx}\ \text{cm}^{-1}\ \text{GPa}^{-1}, \tag{1}$$

$$\varepsilon_{xx} = \sigma_{xx} / \left[\left(C_{11} + C_{12} \right) - 2C_{13}^{\ 2} / C_{33} \right], \tag{2}$$

where $\Delta\omega$ is the Raman shift, σ_{xx} is the stress, and C_{ij} are the elastic constants of GaN (C_{11} = 390 GPa, C_{12} = 145 GPa, C_{13} = 106 GPa, and C_{33} = 398 GPa), which give a proportionality factor of 478 GPa. [14] Raman spectroscopy shows a compressive strain (-0.107%) in MQW-Al_2O_3 and tensile strain (+0.088%) in MQW-Si. These residual strains reflect the type of lattice mismatch between GaN and the substrate: -16.1% for GaN on Al_2O_3 and +17% for GaN on Si.[2] The total difference in the strain of the GaN layers of the samples (~ 0.2%) implies the InGaN quantum wells on the surface should also experience a different level of compressive strain. The reduction in the compressive strain in the InGaN wells on MQW-Si explains the reduction in the QCSE and the observed differences in micro PL.

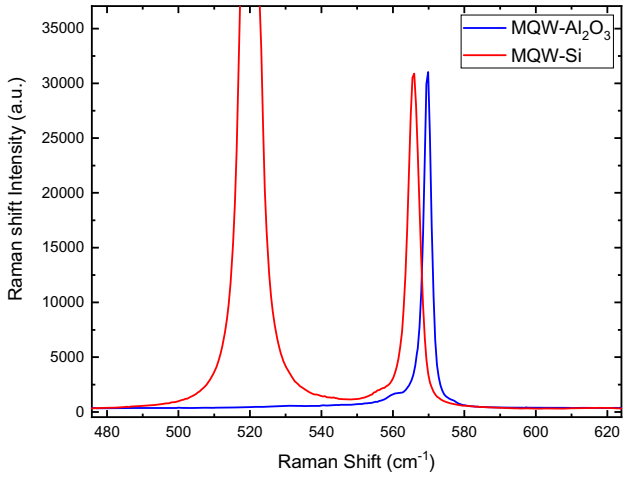

Figure 4. Raman spectra of (blue) MQW-Al_2O_3 and (red) MQW-Si.

Tapping mode AFM is conducted on the samples to quantify the crystal quality at the surface. Figure 5 shows 5 µm × 5 µm AFM scans of (a) MQW-Al_2O_3 and (b) MQW-Si. The surface of MQW-Al_2O_3 shows step-flow terraces with atomic step heights of ~ 3 Å, a threading dislocation density of ~ 2.87×10^8 cm^{-2}, and a root-mean-square (RMS) surface roughness of 1.12 nm. The surface of MQW-Si shows hexagonal spiral hillocks with a mixed type dislocation in the center that are approximately 2 µm apart, a threading dislocation density of ~ 3.20×10^8 cm^{-2}, and a RMS roughness of 0.51 nm.[15] Due to the different type of strain experienced by the GaN layer, they exhibit a different form of epitaxial growth. However, the results from AFM show the crystal quality of MQW-Al_2O_3 is better than MQW-Si, but not by a significant amount.

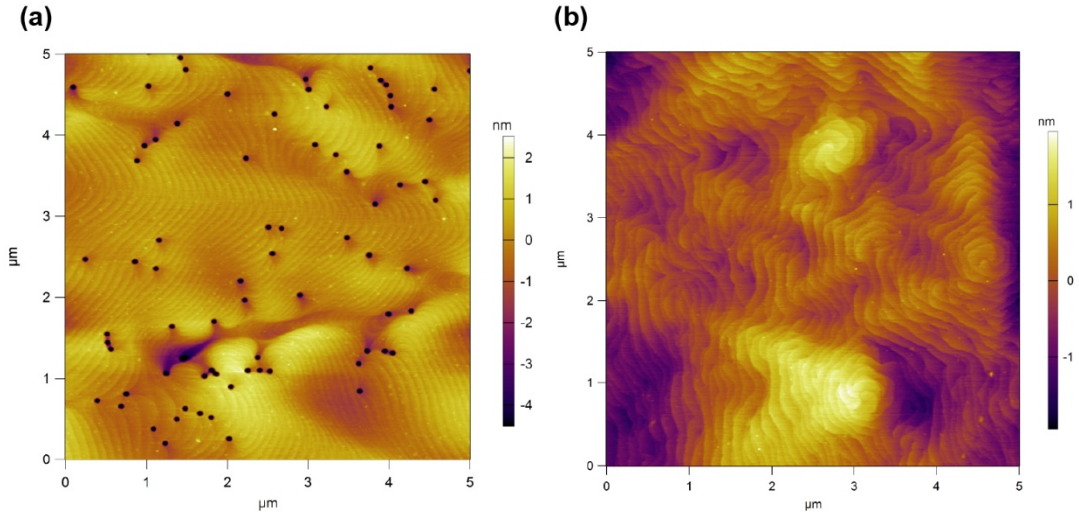

Figure 5. 5 µm × 5 µm tapping mode AFM scans of (a) MQW-Al_2O_3 and (b) MQW-Si. The surface of MQW-Al_2O_3 shows step-flow terraces, whereas the surface of MQW-Si is populated with hillocks.

Figure 6 shows the temperature dependent PL conducted using a frequency-tripled solid-state laser (λ = 266 nm) with temperature ranging from 1.4 K to 300 K. At 300 K, MQW-Al_2O_3 (Fig. 6a) exhibits InGaN multiple quantum well emission centered at 2.812 eV, whereas MQW-Si (Fig. 6b) is centered at 2.838 eV. As temperature decreases, the position of the MQW emission from MQW-Al_2O_3 first blue shifts to a peak of 2.834 eV at 170 K and then red shifts to stabilize at 2.821 eV at 70 K. This S-shaped emission energy shift has been shown to be the manifestation of the indium clustering as carrier gradually lose the thermal energy required to escape the local shallow energy minima, which cause the carriers to recombine in the less abundant and deeper wells.[16] The MQW emission from MQW-Si on the other hand monotonically increases in energy by 16 meV with decreasing temperature. This behavior is exhibited by almost all semiconductor is explained by the Varshni's coefficient.[17]

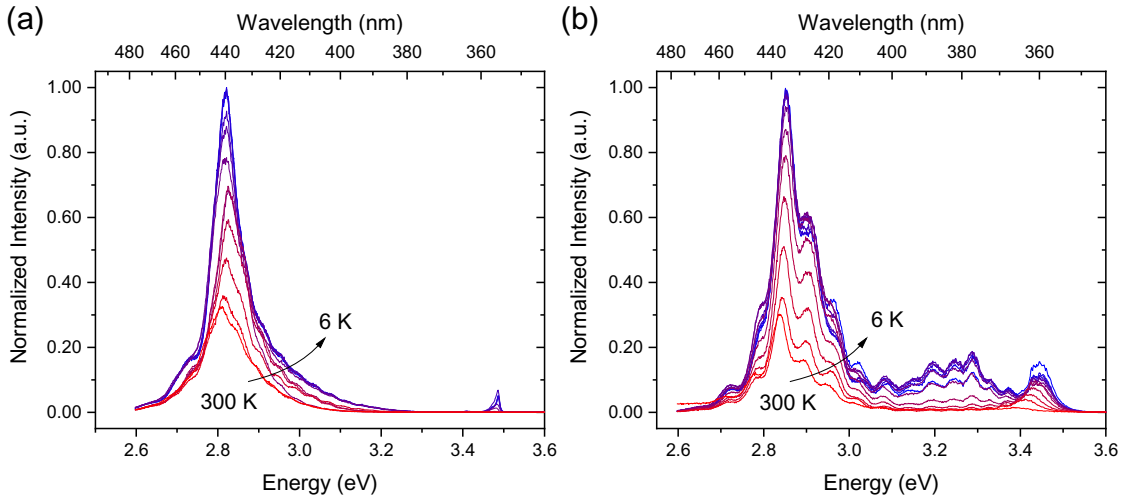

Figure 6. Temperature dependent PL spectra of (a) MQW-Al2O3 and (b) MQW-Si from 6 K (blue) to 300 K (red).

Additional emissions are observed in both samples at temperature lower than 100 K. MQW-Al_2O_3 exhibits a low energy shoulder (2.728 eV) of the main MQW emission and a peak in the ultraviolet range (3.486 eV) that is attributed to the recombination in the GaN layers. The low energy shoulder has been reported to come from the localized indium clusters, which is caused by the phase separation as a result the immiscibility of In- and GaN.[18] The additional emission from MQW-Si at 3.288 eV, along with its LO-phonon replicas that have energies lowered by multiples of 90 meV, originates from the donor-acceptor pair recombination of carriers.[19,20] A NBE emission from GaN at 3.446 eV, which has a shifted bandgap energy due to the strain, is also observed at a higher intensity than that from MQW-Al_2O_3. The presence of a strong DAP recombination in MQW-Si suggests the presence of a high concentration of impurity, which is quite possibly Si, while the stronger GaN NBE emission suggests an inferior carrier confinement in the InGaN quantum wells.

The main emissions from the MQW on Al_2O_3 and Si show an energy difference of 41 meV, which is attributed to the difference in QCSE in the InGaN active layers. The residual strain in the underlying GaN layer has a sizable impact on the magnitude of the compressive strain imposed on the InGaN QWs.

Internal quantum efficiency (IQE) of the samples can be extracted from the temperature dependent PL using:

$$IQE(T) = \frac{I(T)}{I(6\text{ K})}, \tag{3}$$

where *I(T)* is the integrated intensity of the PL emission at temperature *T* while assuming the nonradiative recombinations are frozen at 6 K. MQW-Al_2O_3 and MQW-Si show very similar IQEs of 33 and 30%, respectively, at 300 K. However, the IQE of MQW-Si exceeds that of MQW-Al_2O_3 at all temperatures below 250 K. This indicates that the activation energy of their respective carrier loss mechanism, such as nonradiative recombination centers, are significantly different.

3. DISCUSSION

The carriers in MQW-Al_2O_3 and MQW-Si are shown to behave rather differently even though the MQW structures are grown under the same MOCVD configuration. MQW-Si does not exhibit the intensity-wavelength correlation and the S-shaped shift in the emission energy with decreasing temperature. The lack of these phenomena, which are associated with indium clustering and strong QCSE, indicate the MQW-Si is superior to MQW-Al_2O_3 in indium uniformity and emission stability. These differences are believed to be originated from the different type of residual strain in the GaN layer; the results suggest the tensile strain in the GaN of MQW-Si could be beneficial as it reduces the compressive strain in the InGaN layer. The advantage of this reduction is twofold. First, the reduction in piezoelectric polarization allows the electrons and holes to achieve a greater wavefunction overlap, which should lead to an increased radiative efficiency.[21] This is supported by the IQE analysis, which shows that, despite the lower crystal quality, MQW-Si outperforms MQW-Al_2O_3 at most temperatures and roughly equal at room temperature. Second, tensile strain is shown to be beneficial for indium atom incorporation during MOCVD growth due to strain compensation.[22,23] This is shown by the lack of S-shaped shift in emission energy, low energy shoulders at cryo-temperatures, and the intensity-wavelength correlation. This indicates that the tensile strain allows MQW-Si to incorporate a higher indium content during growth than MQW-Al_2O_3. This demonstrates the possibility of growing MQW-Si with a higher indium mole fraction for the emission of green light.

4. SUMMARY

In conclusion, the carrier dynamics are found to be different in MQW-Al_2O_3 and MQW-Si. The phenomena that are associated with indium clustering observed in MQW-Al_2O_3 are not present MQW-Si. These effects include: intensity-wavelength correlation, band filling, S-shaped emission energy shift, and low energy shoulder at low temperature. The reduction of these behavior in MQW-Si is attributed to the residual tensile strain that originated from the Si substrate. The performance of MQW-Si, as measured by IQE, is on par with MQW-Al_2O_3 at room temperature, and better at temperatures below 250 K despite a thinner overall epitaxial thickness and crystal quality.

REFERENCES

[1] Schmitt, E., Straubinger, T., Rasp, M. and Weber, A. D., "Defect reduction in sublimation grown SiC bulk crystals," Superlattices Microstruct. **40**(4–6 SPEC. ISS.), 320–327 (2006).

[2] Zhu, D., Wallis, D. J. and Humphreys, C. J., "Prospects of III-nitride optoelectronics grown on Si.," Rep. Prog.

Phys. **76**(10), 106501 (2013).
[3] Lee, M., Yang, M., Song, K. M. and Park, S., "InGaN/GaN Blue Light Emitting Diodes Using Freestanding GaN Extracted from a Si Substrate," ACS Photonics **5**(4), 1453–1459 (2018).
[4] Lee, H.-P., Perozek, J., Rosario, L. D. and Bayram, C., "Investigation of AlGaN/GaN high electron mobility transistor structures on 200-mm silicon (111) substrates employing different buffer layer configurations," Sci. Rep. **6**(August), 37588 (2016).
[5] Dadgar, A., Hums, C., Diez, A., Schulze, F., Bläsing, J. and Krost, A., "Epitaxy of GaN LEDs on large substrates: Si or sapphire?," 63550R (2006).
[6] Dadgar, A., Hempel, T., Bläsing, J., Schulz, O., Fritze, S., Christen, J. and Krost, A., "Improving GaN-on-silicon properties for GaN device epitaxy," Phys. Status Solidi Curr. Top. Solid State Phys. **8**(5), 1503–1508 (2011).
[7] Ayers, J. E., "Compliant Substrates for Heteroepitaxial Semiconductor Devices: Theory, Experiment, and Current Directions," J. Electron. Mater. **37**(10), 1511–1523 (2008).
[8] Ryu, H. Y., Jeon, K. S., Kang, M. G., Yuh, H. K., Choi, Y. H. and Lee, J. S., "A comparative study of efficiency droop and internal electric field for InGaN blue lighting-emitting diodes on silicon and sapphire substrates," Sci. Rep. **7**(April), 44814 (2017).
[9] Woo, S. Y., Gauquelin, N., Nguyen, H. P. T., Mi, Z. and Botton, G. A., "Interplay of strain and indium incorporation in InGaN/GaN dot-in-a-wire nanostructures by scanning transmission electron microscopy," Nanotechnology **26**(34) (2015).
[10] Liu, R., McCormick, C. and Bayram, C., "Comparison of Structural and Optical Properties of Blue Emitting In0.15Ga0.85N/GaN Multi-Quantum-Well Layers Grown on Sapphire and Silicon Substrates," AIP Adv., under review (2019).
[11] Kazlauskas, K., Tamulaitis, G., Mickevičius, J., Kuokštis, E., Žukauskas, A., Cheng, Y.-C. C., Wang, H.-C. C., Huang, C.-F. F. and Yang, C. C., "Excitation power dynamics of photoluminescence in InGaN/GaN quantum wells with enhanced carrier localization," J. Appl. Phys. **97**(1), 013525 (2005).
[12] Wang, T., Nakagawa, D., Wang, J., Sugahara, T. and Sakai, S., "Photoluminescence investigation of InGaN/GaN single quantum well and multiple quantum wells," Appl. Phys. Lett. **73**(24), 3571–3573 (1998).
[13] Tripathy, S., Chua, S. J., Chen, P. and Miao, Z. L., "Micro-Raman investigation of strain in GaN and AlxGa1-xN/GaN heterostructures grown on Si(111)," J. Appl. Phys. **92**(7), 3503–3510 (2002).
[14] Polian, A., Grimsditch, M. and Grzegory, I., "Elastic constants of gallium nitride," J. Appl. Phys. **79**(6), 3343–3344 (1996).
[15] Heying, B., Tarsa, E. J., Elsass, C. R., Fini, P., DenBaars, S. P. and Speck, J. S., "Dislocation mediated surface morphology of GaN," J. Appl. Phys. **85**(9), 6470–6476 (1999).
[16] Cho, Y., Gainer, G. H., Fischer, a J., Song, J. J., Keller, S., Mishra, U. K. and DenBaars, S. P., "'S-shaped' temperature-dependent emission shift and carrier dynamics in InGaN/GaN multiple quantum wells," Appl. Phys. Lett. **73**(10), 1370–1372 (1998).
[17] Varshni, Y. P., "Temperature dependence of the energy gap in semiconductors," Physica **34**(1), 149–154 (1967).
[18] Gačević, Ž., Das, A., Teubert, J., Kotsar, Y., Kandaswamy, P. K., Kehagias, T., Koukoula, T., Komninou, P. and Monroy, E., "Internal quantum efficiency of III-nitride quantum dot superlattices grown by plasma-assisted molecular-beam epitaxy," J. Appl. Phys. **109**(10) (2011).
[19] Reshchikov, M. A., Zafar Iqbal, M., Park, S. S., Lee, K. Y., Tsvetkov, D., Dmitriev, V. and Morkoç, H., "Persistent photoluminescence in high-purity GaN," Phys. B Condens. Matter **340**–**342**, 444–447, North-Holland (2003).
[20] Azuhata, T., Sota, T., Suzuki, K. and Nakamura, S., "Polarized Raman spectra in GaN," J. Phys. Condens. Matter **7**(10), L129–L133 (1995).
[21] Monavarian, M., Rashidi, A., Aragon, A. A., Nami, M., Oh, S. H., Denbaars, S. P. and Feezell, D., "Trade-off between bandwidth and efficiency in semipolar (2021) InGaN/GaN single- and multiple-quantum-well light-emitting diodes," Appl. Phys. Lett. **112**(19) (2018).
[22] Johnson, M. C., Bourret-Courchesne, E. D., Wu, J., Liliental-Weber, Z., Zakharov, D. N., Jorgenson, R. J., Ng, T. B., McCready, D. E. and Williams, J. R., "Effect of gallium nitride template layer strain on the growth of InxGa1-xN/GaN multiple quantum well light emitting diodes," J. Appl. Phys. **96**(3), 1381–1386 (2004).
[23] Ryou, J.-H., Douglas Yoder, P., Liu, J., Lochner, Z., Kim, H., Jin Kim, H. and D. Dupuis, R., "Control of Quantum-Confinement Stark Effect in InGaN-Based Quantum Wells," IEEE J. Sel. Top. Quantum Electron. Vol. 15, No. 4 **15**(4), 1080–1091 (2009).